Cell

Dicer-Independent Primal RNAs Trigger RNAi and Heterochromatin Formation

Mario Halic[1] and Danesh Moazed[1,2,*]
[1]Department of Cell Biology
[2]Howard Hughes Medical Institute
Harvard Medical School, Boston, MA, 02115, USA
*Correspondence: danesh@hms.harvard.edu
DOI 10.1016/j.cell.2010.01.019

SUMMARY

Assembly of fission yeast pericentromeric heterochromatin and generation of small interfering RNAs (siRNAs) from noncoding centromeric transcripts are mutually dependent processes. How this interdependent positive feedback loop is first triggered is a fundamental unanswered question. Here, we show that two distinct Argonaute (Ago1)-dependent pathways mediate small RNA generation. RNA-dependent RNA polymerase complex (RDRC) and Dicer act on specific noncoding RNAs to generate siRNAs by a mechanism that requires the slicer activity of Ago1 but is independent of pre-existing heterochromatin. In the absence of RDRC or Dicer, a distinct class of small RNAs, called primal small RNAs (priRNAs), associates with Ago1. priRNAs are degradation products of abundant transcripts, which bind to Ago1 and target antisense transcripts that result from bidirectional transcription of DNA repeats. Our results suggest that a transcriptome surveillance mechanism based on random association of RNA degradation products with Argonaute triggers siRNA amplification and heterochromatin assembly within DNA repeats.

INTRODUCTION

Small RNAs play central and conserved roles in gene regulation and in maintaining the stability of repetitive DNA sequences associated with transposons and retroelements (Aravin et al., 2007; Baulcombe, 2004; Ghildiyal and Zamore, 2009; Mello and Conte, 2004). Small interfering RNAs (siRNAs) and microRNAs interact with target RNAs by base pairing interactions and promote either translational inhibition or degradation of complementary RNAs in a posttranscriptional mode of RNA interference (RNAi) (Ghildiyal and Zamore, 2009; Hutvagner and Simard, 2008). In the fission yeast *Schizosaccharomyces pombe*, the ciliate *Tetrahymena thermophila*, plants, and *Drosophila*, small RNA pathways also act at the chromatin or DNA level (Moazed, 2009).

RNAi is triggered by double-stranded RNA (dsRNA), which is processed into siRNAs by Dicer (Hannon, 2002). siRNAs are loaded onto Argonaute and direct the inactivation of target RNAs by guiding the RNA-induced silencing complex (RISC) or the RNA-induced transcriptional silencing (RITS) complex to specific target sequences (Hammond et al., 2000; Verdel et al., 2004). In the *S. pombe* RITS complex, Argonaute interacts with two additional proteins, Tas3 and Chp1. Tas3, a glycine and tryptophan (GW) motif-containing protein, links Ago1 to Chp1 (Debeauchamp et al., 2008). Chp1 is a chromodomain-containing protein and specifically interacts with histone H3 lysine 9 (H3K9) di- or trimethylated nucleosomes (Partridge et al., 2002; Schalch et al., 2009), which are a hallmark of heterochromatin. RITS can therefore associate with chromatin through base-pairing interactions of siRNAs in Ago1 with nascent transcripts and interaction of Chp1 with H3K9 methylated nucleosomes (Verdel et al., 2004). This leads to the recruitment of the Clr4-Rik1-Cul4 (CLRC) methyltransferase/ubiquitin ligase complex to chromatin, additional cycles of H3K9 methylation, and recruitment of two other chromodomain proteins, Swi6 and Chp2, which are the fission yeast HP1 homologs. In addition to RITS, *S. pombe* contains an Argonaute siRNA chaperone (ARC) complex, in which Ago1 is associated with the Arb1 and Arb2 proteins and duplex siRNAs (Buker et al., 2007).

In fission yeast, nematodes and plants, the silencing signal is amplified by the activity of RNA-dependent RNA polymerase (RdRP) (Henderson and Jacobsen, 2007; Motamedi et al., 2004; Sijen et al., 2001; Smardon et al., 2000). The fission yeast RdRP, Rdp1, is associated with two conserved proteins, Hrr1 and Cid12, in a functional RNA-dependent RNA polymerase complex (RDRC) (Motamedi et al., 2004). Hrr1 has high similarity to DEAD box RNA helicases, which are required for RNAi mediated silencing in plants, *C. elegans*, and *Drosophila* (Tomari et al., 2004). Cid12, a nucleotidyltransferase domain-containing protein, belongs to a Trf4/Trf5 family of poly(A) polymerases, and its homologs are required for RNAi-mediated silencing in other eukaryotes (Chen et al., 2005; Lee et al., 2009).

In the nascent transcript cycle described above, the RNAi machinery localizes to chromatin-bound transcripts and mediates their processing into siRNAs, which promote heterochromatin assembly and the generation of additional siRNAs. However, it remains unclear how siRNA generation and heterochromatin assembly are initiated in the first place, since the cycle begins with an siRNA-programmed RITS. It has been suggested

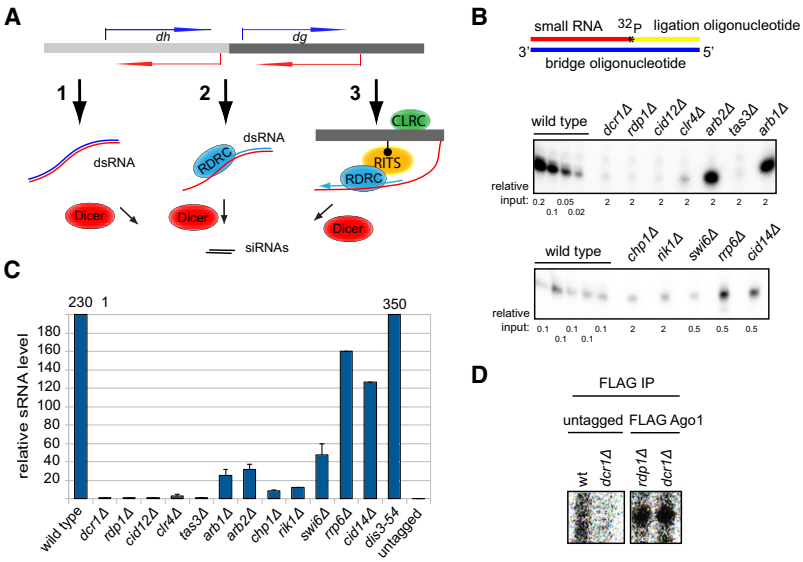

Figure 1. Detection of Small RNAs in RNAi and Heterochromatin Mutant Backgrounds with Splinted Ligation

(A) Possible models for biogenesis of initial siRNAs from centromeric repeats, including dsRNA resulting from bidirectional transcription (1), RDRC recognition of specific sequences (2), and RITS/RDRC recruitment by pre-existing H3K9 methylation (3).

(B) Detection of Argonaute-associated centromeric small RNAs in wild-type and the indicated mutant cells by splinted ligation. Bridge oligonucleotides corresponding to eight different centromeric siRNAs mapping to both dg and dh transcripts were used. Note that different amounts of Ago1-associated small RNAs, indicated as relative input, were used for different strains and normalized to the levels in wild-type cells. Note different exposure times for the upper and lower panels.

(C) Quantification of the splinted ligation data by Quantity One software. Splinted ligation experiments were performed with three or more biological replicates, and standard deviations are shown. Small RNA quantification for *dis3-54* was done twice, and error bars represent deviation from the mean. *rrp6*Δ and *cid14*Δ data are based on only one experiment and are consistent with previous findings. The signal for *dcr1*Δ was set to 1 and enrichment over *dcr1*Δ is shown.

(D) Detection of Argonaute-associated centromeric small RNAs by splinted ligation in *dcr1*Δ and *rdp1*Δ cells. In untagged purifications from wild-type and *dcr1*Δ cells no centromeric small RNAs were detected.

See also Figure S1.

that trigger centromeric siRNAs are produced from the processing of double-stranded RNA (dsRNA), which may form either by base pairing of sense and antisense centromeric transcripts or by RDRC-dependent activity on specific centromeric RNAs (Figure 1A). In an alternative model, low levels of histone H3K9 methylation, which are present in RNAi mutants (Noma et al., 2004; Sadaie et al., 2004), have been suggested to act upstream of RNAi by recruiting the RITS and RDRC complexes to centromeric repeats to initiate siRNA generation and the amplification of H3K9 methylation (Figure 1A). No evidence in support of these models has yet been obtained.

In this report, we use biochemical and high-throughput sequencing approaches to examine the mechanisms that mediate small RNA generation from the fission yeast centromeric repeat sequences. The higher sensitivity of the methods used in our experiments allows us to detect centromeric small RNAs in mutant backgrounds that had been considered to lack siRNAs. We demonstrate the existence of two Ago1-dependent pathways that mediate the generation of different levels of small RNAs from centromeric repeat sequences. First, small RNA profiles in heterochromatin mutants indicate that the amplification of siRNAs can occur independently of H3K9 methylation and involves RDRC and Dicer activity on specific noncoding RNAs. This amplification requires the slicer activity of Ago1, suggesting that the Ago1-associated small RNAs target RDRC to centromeric transcripts. Second, we describe a distinct class of small RNAs, called primal small RNAs (priRNAs), which are generated independently of Dicer or RDRC. priRNAs appear to be degradation products of abundant genome-wide transcripts. We provide evidence that priRNAs act through Argonaute to mediate low levels of H3K9 methylation at pericentromeric repeats and propose that they trigger RDRC/Dicer-dependent siRNA amplification from antisense centromeric RNAs. In addition, we provide evidence that siRNAs undergo processing at their 3′ ends, which involves the addition of untemplated nucleotides by the Cid12 and Cid14 nucleotidyltransferases and trimming, most likely mediated by the exosome. Our results suggest that a transcriptome surveillance mechanism based on the random association of small RNAs with Argonautes triggers RNAi-mediated heterochromatin formation within DNA repeats.

RESULTS

Detection of Ago1-Bound Small RNAs in RNAi and Heterochromatin Mutants

Several different models can explain how trigger siRNAs are first generated from centromeric transcripts (Figure 1A). In model 1, siRNAs are generated by Dicer-mediated processing of dsRNA that is formed from base pairing of sense and antisense centromeric transcripts resulting from bidirectional transcription. In model 2, RDRC recognizes specific features of centromeric RNAs and synthesizes the initial dsRNA substrate for Dicer. In model 3, pre-existing H3K9 methylation recruits RITS and RDRC to transcripts in centromeric regions in an siRNA-independent manner. These models make specific predictions about siRNA levels in different mutant backgrounds. However, previous studies employing 3′ end labeling and northern blotting, while showing a requirement for RDRC/Dicer and heterochromatin proteins in centromeric siRNA generation, have not detected differences in siRNA levels in the respective mutant backgrounds (Bühler et al., 2006; Motamedi et al., 2004; Noma et al., 2004; Verdel et al., 2004).

In order to distinguish between the above models, we used the sensitive splinted ligation detection assays to determine siRNA

levels in FLAG-Ago1 purifications from Dicer, RDRC, and heterochromatin mutant cells (Figure 1B, Figure S1A available online). In splinted ligation detection assays, small RNAs are ligated to a 5′ ^{32}P-labeled oligonucleotide, directed by a specific bridge oligonucleotide, and the detection has been reported to be approximately 50-fold more sensitive than northern blotting for small RNA (Maroney et al., 2008). Using this method, we observed >100-fold reduction in siRNA levels in *dcr1*Δ, *rdp1*Δ, *cid12*Δ, *clr4*Δ, and *tas3*Δ cells (Figures 1B and 1C, Figure S1B). siRNA levels were also greatly reduced in cells lacking the Arb1 and Arb2 subunits of the ARC complex, the Chp1 subunit of the RITS complex, the Rik1 subunit of the CLRC methyltransferase complex, and the Swi6/HP1 protein (Figures 1B and 1C). In contrast to previous studies, we detected small RNAs in *dcr1*Δ, *rdp1*Δ, and several other mutant backgrounds that were consistently above control FLAG immunoprecipitations from either untagged wild-type or *dcr1*Δ cells (Figures 1C and 1D, Figure S1B). In *rdp1*Δ and *dcr1*Δ cells, small RNA levels were similar, suggesting that few or no siRNAs were produced from dsRNA resulting from the base pairing of sense and antisense centromeric transcripts, strongly arguing against model 1 (Figures 1B–1D, Figure S1B). Furthermore, the presence of small RNAs in *dcr1*Δ cells suggested the existence of a Dicer-independent small RNA generation mechanism in *S. pombe*.

High-Throughput Sequencing of Ago1-Bound Small RNAs Reveals 3′ End Processing of siRNAs by Nucleotidyltransferases

The splinted ligation results suggested that high-throughput sequencing of Ago1-associated small RNAs from mutant cells may provide additional information about the factors and centromeric sequences that mediate small RNA biogenesis. Using Illumina sequencing, we obtained between one and six million reads for 5′-monopohosphate containing small RNAs associated with FLAG-Ago1 in wild-type and mutant cells (Figures 2A and 2B, Table S1). Consistent with previous results (Bühler et al., 2008; Cam et al., 2005), in wild-type cells, the majority of small RNAs mapped to both DNA strands of the centromeric *dg* and *dh* repeats, present in all three chromosomes, and to the *IRC3* repeat elements, which flank the *dg* and *dh* repeats of chromosome 3 (Figure 2B, Figure S2). In addition, we observed a striking correlation between small RNA peaks and the occurrence of both sense and antisense transcription (Figure S2A). The majority of the remaining small RNA reads mapped to the sense strand of rRNAs, tRNAs, and mRNAs (Figure 2A). Consistent with the splinted ligation results (Figures 1B–1D), in *dcr1*Δ, *rdp1*Δ, and *cid12*Δ cells, centromeric small RNAs were severely reduced but not eliminated (Figures 2A and 2B). The residual small RNAs in the above mutant backgrounds had a similar 5′ nucleotide preference and length distribution as wild-type siRNAs suggesting that this preference was dictated by Ago1 binding (Figure S2B and data not shown).

In *cid12*Δ cells, about 10-fold more centromeric siRNAs were present compared to *dcr1*Δ or *rdp1*Δ cells (Figures 2A and 2B, zoomed graphs), suggesting that low levels of siRNA could be generated independently of Cid12. Moreover, overexpression of Rdp1 from the strong *nmt1* promoter in *cid12*Δ cells restored centromeric dg and dh siRNAs to near wild-type levels (Figure 2C, Figures S2C and S2D) and restored silencing of an *imr1R::ura4*$^{+}$ centromeric reporter gene (Figure 2D), indicating that the resulting siRNAs were functional. However, Rdp1 overexpression failed to restore the normally abundant siRNAs corresponding to the *IRC3* repeats of chromosome 3, indicating an essential role for Cid12 in RNAi at this element (Figure S2C). Furthermore, Rdp1 overexpression did not suppress the silencing defect of other RNAi mutant cells (Figure S2E), suggesting that the mechanism of this suppression was specifically related to a partial bypass of Cid12 function in the RDRC complex.

Cid12 is one of two nucleotidyltransferase enzymes that are required for efficient RNAi in *S. pombe* (Motamedi et al., 2004). Cid14, another enzyme in this family, is a component of the TRAMP polyadenylation complex and is required for efficient siRNA generation and heterochromatic gene silencing (Bühler et al., 2007). Although previous evidence suggests that Cid12 and Cid14 perform overlapping and/or competing functions (Bühler et al., 2007), it has been unclear whether they target long noncoding RNAs or siRNAs. We noticed that a strikingly high percentage of Ago1-bound small RNAs contained mismatches at their 3′ last two nucleotides (Figure 2E, positions 0 and −1 from the 3′ end), raising the possibility that Cid12 and/or Cid14 extended the 3′ ends of these small RNAs in a template independent manner. In wild-type cells, the mismatch residues were A, U, or C (Figure 2F), but both the frequency and identity of the mismatches were altered in mutant backgrounds (Figures 2E and 2F). In both *cid12*Δ and *cid14*Δ cells, the frequency of mismatches at the last two 3′ nucleotide positions of total and centromeric small RNA populations was reduced (Figure 2E), suggesting that small RNAs were targeted by the nucleotidyltransferase activities of Cid12 and Cid14. Finally, we observed changes in the identity of mismatched residues in mutant backgrounds (Figure 2F, Figure S2F). In *dcr1*Δ and *cid12*Δ cells, the mismatch residue was primarily A (Figure 2F), suggesting that in the absence of heterochromatin-dependent processing, small RNAs become targets for Cid14, which has primarily polyadenylation activity in vitro (Bühler et al., 2007). In contrast, in *cid14*Δ cells, mismatches were primarily U or A, and to a lesser extent C (Figure 2F), suggesting a role for another nucleotidyltransferase, possibly Cid12.

To address the possibility that Cid12 has nucleotidyltransferase activity, we reconstituted RDRC complexes containing active site mutations in either the Cid12 or Rdp1 subunits so that we could distinguish Cid12 activity from Rdp1 activity. We were unable to detect any adenylation activity in purified Cid12 preparations (Figure 2G, lane 5). However, Cid12 had robust adenylation activity when assembled into the RDRC complex, containing either wild-type Rdp1 or catalytically inactive Rdp1D903A (Figure 2G, lanes 1, 3, and 4), suggesting that Cid12 activity was allosterically regulated. The RNA template, rather than the synthesized second strand, was the target of adenylation by Cid12, since adenylation did not require the dsRNA synthesis activity of Rdp1 and the product migrated as single stranded during native polyacrylamide gel electrophoresis (Figure 2G). We confirmed this observation by subsequent treatment of the reaction with terminator exonuclease, which degrades the 5′-monophosphate-containing input RNA

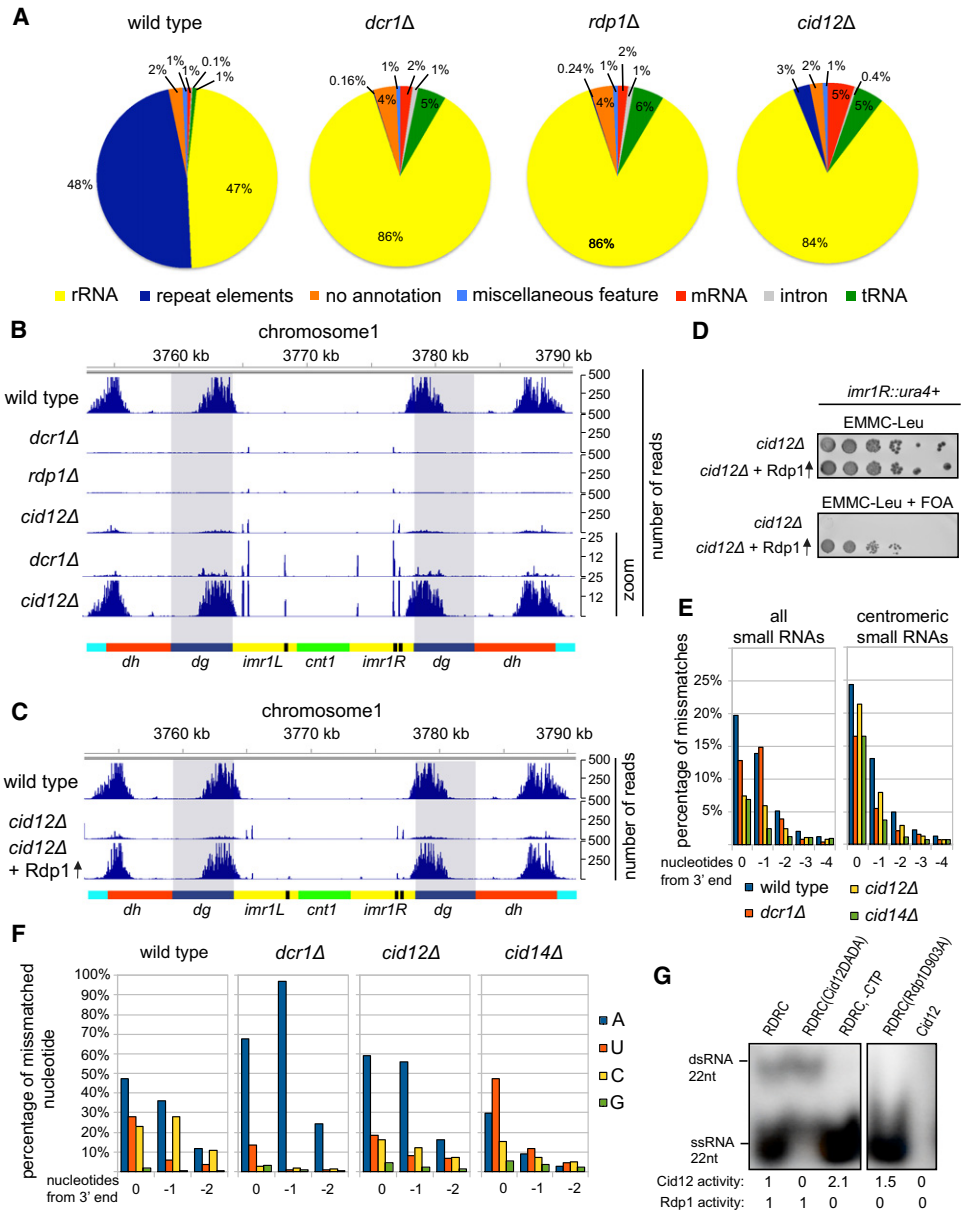

Figure 2. Roles of Dicer and RDRC in Small RNA Generation

(A) *S. pombe* Ago1-associated small RNAs were analyzed by high-throughput sequencing from wild-type, *dcr1*Δ, *rdp1*Δ, and *cid12*Δ cells, and classified as indicated below the pie charts. Pie charts illustrate percentages for the individual small RNA classes relative to the total number of small RNA reads for each strain.

(B) Small RNA reads in wild-type and the indicated mutant cells were plotted over centromeric repeat region of chromosome 1. The location of the centromere (*cnt1*, green), the *imr* repeats (*imr1L* and *imr1R*, yellow), tRNAs (black), the *dg* (blue), and *dh* (red) repeats are indicated below the siRNA peaks. Chromosome coordinates are indicated above the peaks. Scale bars on the right denote small RNA reads numbers normalized per one million reads.

(C) Small RNA reads in wild-type, *cid12*Δ and *cid12*Δ overexpressing Rdp1. Shaded areas highlight the *dg* repeats.

(D) Silencing assay showing that Rdp1 overexpression rescues the *cid12*Δ loss of silencing phenotype of a *imr1R::ura4*$^{+}$ reporter gene. Plating efficiency and silencing are assayed by growth on complete selective (EMMC-Leu) and 5-Fluoroorotic acid (FOA) medium, respectively.

(E) Percentage of mismatched nucleotides for all small RNAs (sRNAs) and centromeric small RNAs in wild-type, *dcr1*Δ, *cid12*Δ and *cid14*Δ cells. The last 5 nt are shown from 3′ end of small RNA. 0 denotes the last nucleotide, −1 the nucleotide prior to the last.

(F) Identity of mismatched nucleotides in small RNAs in wild-type, *dcr1*Δ, *cid12*Δ, and *cid14*Δ cells. As in (E), mismatched nucleotides are shown from 3′ end of small RNAs.

(G) Autoradiograph of native polyacrylamide gel showing the Cid12 and Rdp1 activities on a 22 nt single-stranded RNA (ssRNA) template using ^{32}P-ATP incorporation. Cid12 products migrate as ssRNA, whereas Rdp1 products migrate as double-stranded RNA (dsRNA). No Rdp1 dsRNA synthesis activity was detectable in absence of CTP or with the catalytically inactive Rdp1-D903A enzyme.

See also Figure S2.

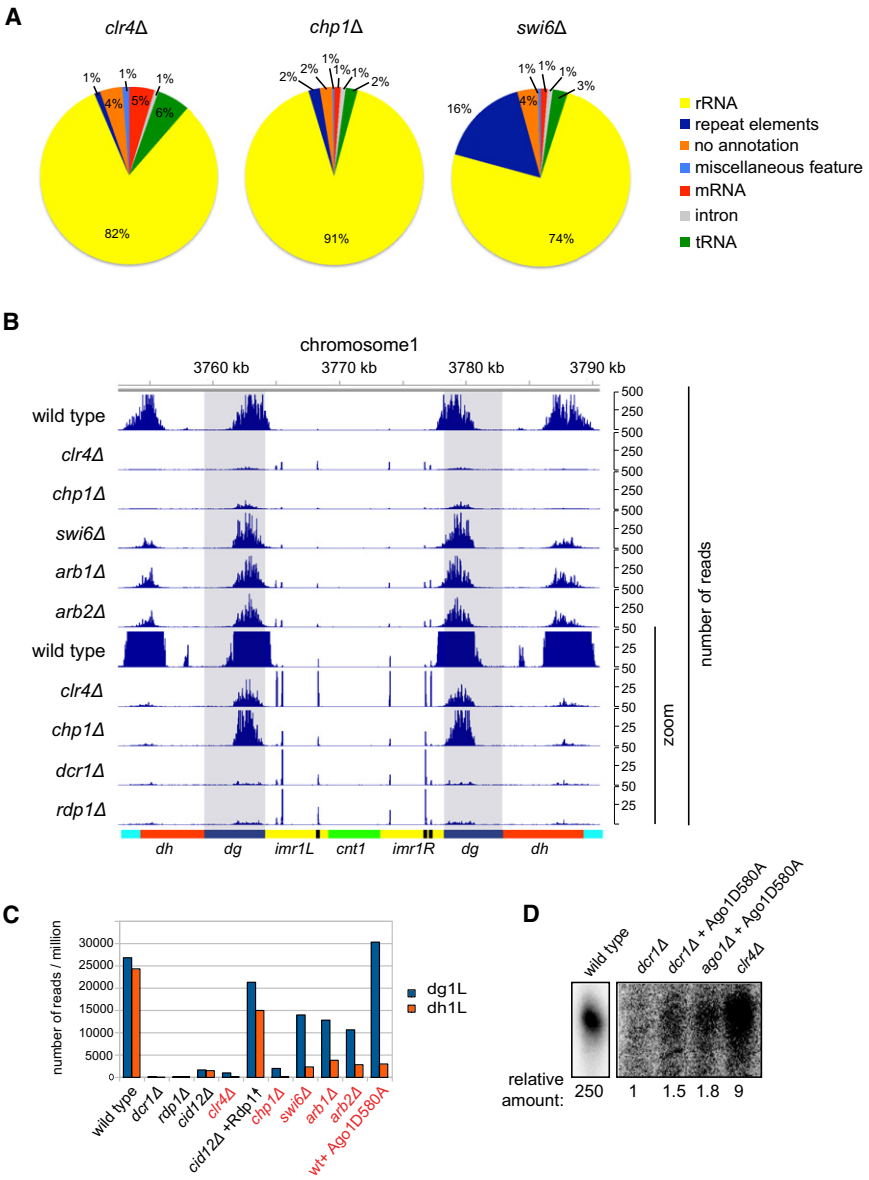

Figure 3. Heterochromatin-Independent siRNA Generation from dg Transcripts

(A) High-throughput sequencing of small RNAs from the *clr4*Δ, *chp1*Δ, and *swi6*Δ cells. Pie charts illustrate percentages for the individual small RNA classes relative to the total number of small RNA reads for each strain, classified as indicated.

(B) Small RNA reads from wild-type and the indicated mutant cells are plotted over centromeric repeat region of chromosome 1, at 10× zoom. (The lower part of panel B shows that in *chp1*Δ and *clr4*Δ cells, dg siRNAs levels are much higher than dh siRNA levels.)

(C) Number of small RNA reads mapping to *dg1L* and *dh1L* in indicated cells. Small RNA read numbers were normalized per one million reads.

(D) Splinted ligation detection of small RNAs associated with Ago1 and Ago1D580A in wild-type, *dcr1*Δ, *ago1*Δ, and *clr4*Δ cells. Five different centromeric small RNAs mapping to dg transcripts were assayed.

See also Figure S3.

RDRC-Dependent Amplification of dg Centromeric siRNAs in the Absence of Heterochromatin

The observation that siRNAs were present in heterochromatin mutant cells prompted us to examine their distribution in these mutants by high-throughput sequencing. Consistent with the splinted ligation results (Figure 1), sequencing showed that siRNA levels were greatly reduced in *clr4*Δ and *chp1*Δ cells and to a lesser extent in *swi6*Δ cells (Figures 3A and 3B). In *clr4*Δ cells, H3K9 methylation is completely abolished; however, we were able to detect relatively high levels of siRNAs from centromeric *dg* repeats, while small RNA reads mapping to *dh* repeats were present at similar levels to *dcr1*Δ and *rdp1*Δ cells (Figure 3B, Figure S3A). Although dg siRNAs in *clr4*Δ cells were amplified approximately 10-fold in an H3K9 methylation- and heterochromatin-independent manner, their generation remained Dicer and RDRC dependent (Figure 3B, Figures S3A and S3B).

In *clr4*Δ, *swi6*Δ, and *chp1*Δ cells, *imr* siRNAs, as well as the *IRC3* siRNAs, were also nearly abolished (Figure 3B, Figure S3A). siRNAs appear to spread from the *dg* element into adjacent *imr1* sequences, likely as a result of processing of transcripts that originate in *dg* and terminate in *imr1* (Figure 3B). siRNA generation from *dh*, *imr*, and *IRC3* elements appeared to be more sensitive to heterochromatin disruption. In *swi6*Δ cells, the reduction in siRNA levels at the *dg* repeats was modest (2-fold), while at the *dh* repeats, siRNA levels were reduced by more than 10-fold (Figures 3A–3C, Figure S3A), consistent with previous studies using *dh*-specific probes for northern blotting (Motamedi et al., 2008). Analysis of small RNA sequences in

substrate but not the 5′-triphosphate-containing Rdp1 product (Pak and Fire, 2007; Sijen et al., 2007). The Cid12 product was completely degraded, indicating that Cid12 modified the 3′ end of the 5′-monophosphate containing RNA substrate (Figure S2G). In contrast to Cid14 and other members of the Trf4/5 family (Bühler et al., 2007; Wang et al., 2008a), Cid12 extended the 3′ end of the RNA substrate by adding only one nucleotide incorporating adenine and less efficiently uracil (Figures S2G and S2H). This observation strongly suggested that Cid12 monoadenylated and remained bound to its RNA substrate, which may help to target the RNA for dsRNA synthesis by the associated Rdp1. Together with the in vivo effects of deleting *cid12*$^{+}$ on the frequency of mismatches at the 3′ ends of Ago1-bound small RNAs, these data suggest that Cid12 adenylates or uridylates small RNAs in vivo.

*arb1*Δ and *arb2*Δ cells revealed a surprisingly similar pattern of distribution to that observed in *swi6*Δ cells (Figure 3B, Figures S3A–S3D), suggesting that these Ago1-associated proteins act in the heterochromatin-dependent siRNA generation pathway. Together, these results identify the centromeric *dg* repeats as heterochromatin-independent RNAi nucleation regions and eliminate a strict requirement for pre-existing heterochromatin in siRNA generation (model 3, Figure 1A).

Ago1 Slicer Activity Is Required for RDRC-Dependent Amplification of siRNAs

We wished to determine whether dg siRNA amplification involved the direct recognition of dg RNAs by the RDRC complex (model 2, Figure 1A) and whether it involved Ago1 or the RITS complex. As shown in Figure 3B (lower zoom graphs), the Chp1 subunit of the RITS complex was not required for accumulation of dg siRNAs; however, the Tas3 subunit was required as small RNA levels in *tas3*Δ and *dcr1*Δ cells were similar (Figures 1B and 1C). This rules out a requirement for the full RITS complex in heterochromatin-independent siRNA generation. Furthermore, using splinted ligation, we found that in cells containing Ago1-D580A, which is defective in slicer activity, dg small RNA levels were similar to that found in *dcr1*Δ cells, and below the levels found in *clr4*Δ cells (Figure 3D). This observation suggests that heterochromatin-independent dg siRNA amplification (model 2, Figure 1A) involves Ago1-mediated slicing or recognition of the dg RNA template and therefore would require a triggering dg small RNA.

Dicer- and RDRC-Independent priRNAs

As noted above, a substantial number of Ago1-associated centromeric small RNAs were present even in *dcr1*Δ and *rdp1*Δ cells (Figures 1–3, Figures S1–S3). Consistent with the splinted ligation results (Figures 1B–1D), the total number of small RNAs was similar in *rdp1*Δ and *dcr1*Δ cells (Figures 4A and 4B, Figure S4A), indicating that the sense and antisense centromeric transcripts do not produce high levels of dsRNA that can be processed into siRNAs by Dicer. The Dicer-independent small RNAs mapped to both strands of the *dg* and *dh* repeats and had a similar overall size and 5′ nucleotide preference as siRNAs in wild-type cells (Figure 4A, Figures S4B and S4C), raising the possibility that they may function like siRNAs. Although Dicer-independent small RNAs originated from rRNAs and tRNAs, as well as abundant mRNA transcripts (Figure 2A), only a small fraction (<1%) mapped with an antisense orientation to known transcripts (Figure 4C, Figures S4D and S4E). Of this antisense fraction, 22% mapped to centromeric *dg* and *dh* elements (Figure 4D), which constitute only 0.4% of the *S. pombe* genome. Furthermore, while 71% of antisense reads map to mRNAs, this fraction is distributed over many mRNA transcripts. The number of antisense small RNA reads per mRNA transcript was therefore negligible compared to the number of antisense small RNAs per dg or dh RNA (Figure 4E). This is due to the fact that high levels of antisense transcription appear to be a unique feature of centromeric repeats in *S. pombe*. In addition the majority of priRNAs mapping to coding regions showed a striking enrichment toward the 3′ ends of annotated transcripts, often overlapping 3′ untranslated sequences or regions just after transcription termination (Figure 4F, Figures S4D and S4E). These observations suggest a relationship between priRNA biogenesis at these regions and RNA processing events associated with transcription termination and also provide further support for the proposal that priRNAs originate from degradation products of single stranded transcripts.

Consistent with the results in Figure 1, showing that Dicer-independent small RNAs were enriched in FLAG pulldowns from FLAG-Ago1 cells compared to untagged control cells, centromeric small RNAs were enriched in Ago1 immunoprecipitations compared to total RNA (Figure 4G). As further tests of specificity, we created a strain with point mutations in the PAZ and MID domains of Ago1 (Wang et al., 2008b) (Ago1-F276A/Y513A/K517A, hereafter referred to as Ago1-A3), which are involved in small RNA binding. Staining for all RNAs with Sybr Green showed that 21–24 nucleotide small RNAs and some larger small RNAs (30–40 nucleotides long) were enriched in Ago1 compared to Ago1-3A immunoprecipitations from *dcr1*Δ cells (Figure 4H), providing further evidence for the specific association of Dcr1-independent small RNAs with Ago1. As expected, Ago1-A3 mutations abolished heterochromatin-dependent gene silencing of an *otr1R::ura4*$^{+}$ reporter gene (Figure 4I). Furthermore, in contrast to wild-type FLAG-Ago1 and FLAG-Ago1-F276A pulldowns, using the splinted ligation method, we did not detect any centromeric small RNAs in FLAG-Ago1-A3 pulldowns, which excluded contamination as a source of small RNAs in FLAG-Ago1 purifications from *dcr1*Δ and other mutant cells (Figure 4J). We also did not detect small RNA reads from the *IRC3* element in *dcr1*Δ (Figure S4A), even though siRNAs originating from this element are the most abundant class in wild-type cells (Figure S3A), further ruling out cross-contamination. We refer to these Dicer-independent small RNAs as primal small RNAs (priRNAs, see below).

Role for priRNAs in Promoting Histone H3K9 Methylation

We next tested whether priRNAs could function through Ago1 to influence heterochromatin assembly at centromeric repeats. It has previously been shown that H3K9 methylation at centromeric repeats is greatly diminished, but not eliminated, in RNAi mutant cells (Noma et al., 2004; Verdel et al., 2004; Volpe et al., 2002). If priRNAs, which are produced independently of Dicer (and Rdp1 as described later), were able to act through Ago1 and/or the RITS complex to promote H3K9 methylation, we would expect a greater defect in H3K9 methylation in *ago1*Δ cells compared to *dcr1*Δ or *rdp1*Δ cells. To test this possibility, we analyzed H3K9 methylation at several locations within the centromeric *dg* repeats (designated dgG, dgB, dgH, and dgF, Figure 5A). Indeed, using chromatin immunoprecipitation (ChIP), we consistently observed that H3K9 methylation levels at the centromeric *dg* repeats were lower in *ago1*Δ compared to *dcr1*Δ or *rdp1*Δ cells (Figures 5B–5E, Figures S5A–S5E). H3K9 methylation in *ago1*Δ cells was in general close to the background observed in *clr4*Δ cells (Figures 5B–5E, Figures S5A–S5E), suggesting that the previously reported RNAi-independent H3K9 methylation at centromeres was mostly Ago1 dependent.

To determine whether Ago1-dependent, but Dcr1-independent, H3K9 methylation required the PAZ and MID domains of Ago1, which were required for priRNA binding (Figure 4J), we

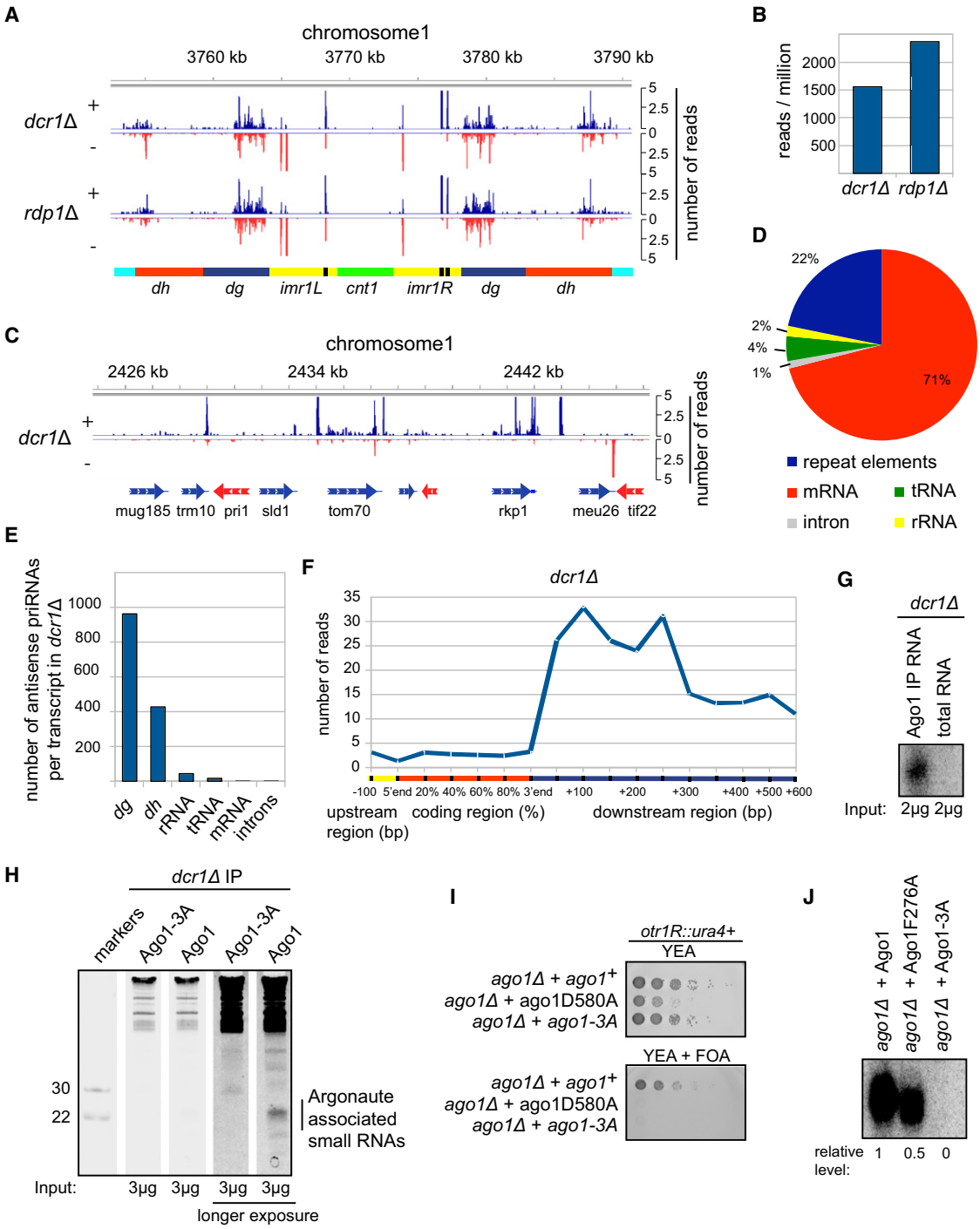

Figure 4. priRNAs Primarily Target the Centromeric Repeats and Require the PAZ/MID Domains for Binding to Ago1

(A) Small RNA reads from *dcr1*Δ and *rdp1*Δ cells are plotted over centromeric region on chromosome 1 in a strand specific way (blue, + strand; red, − strand). Small RNAs in *dcr1*Δ cells are referred to as priRNAs.

(B) Number of centromeric small RNA reads in *dcr1*Δ and *rdp1*Δ cells. Small RNA read numbers were normalized per one million reads.

(C) Small RNA densities from *dcr1*Δ are plotted over a selected euchromatic region on chromosome 1 in a strand-specific way. Note that higher number of reads is often present after the 3′ end of mRNA transcripts.

(D) Classification of antisense priRNAs, as indicated next to the pie charts. Pie charts illustrate the percentages of the individual priRNA classes relative to the total number of antisense priRNAs. Twenty-two percent of antisense priRNAs map to repeat elements.

(E) Antisense small RNA reads for each class are normalized to the number of transcripts they may target. Antisense priRNAs target mainly centromeric dg and dh transcripts.

examined H3K9 methylation levels in cells containing Ago1-3A (Figure 5C). H3K9 methylation levels in Ago1-3A and *ago1*Δ cells were similar, indicating that the ability of Ago1 to promote Dicer-independent H3K9 methylation required its small RNA binding domain. Since in the absence of Dcr1 only priRNAs are present in Ago1, this observation supports a role for priRNAs in promoting low levels of H3K9 methylation.

To determine whether priRNA-mediated H3K9 methylation required the RITS complex, we compared H3K9 methylation levels in *ago1*Δ cells with cells lacking the Chp1 or Tas3 subunits of the RITS complex. H3K9 methylation levels in *chp1*Δ, *tas3*Δ, and *dcr1*Δ*tas3*Δ cells were higher than the levels in *ago1*Δ and close to those found in *dcr1*Δ cells (Figures 5C and 5E), suggesting that Ago1 promoted H3K9 methylation independently of Chp1 and Tas3, although less efficiently. Furthermore, we have previously shown that the slicer-defective Ago1-D580A mutant has a dominant negative effect on heterochromatin formation and inhibits H3K9 methylation even in the presence of a wild-type Ago1 (Buker et al., 2007). Here, we also found that Ago1-D580A was not able to promote Dcr1-independent H3K9 methylation (Figure 5D). Together, our findings reveal a correlation between small RNA levels and their ability to bind to Ago1 with centromeric H3K9 methylation levels (Figure 5E). Thus, H3K9 methylation levels, which are the highest in wild-type cells, are reduced in cells that cannot amplify small RNAs or couple this amplification to chromatin targeting (6- to 9-fold reduction in *dcr1*Δ, *rdp1*Δ, *chp1*Δ, *tas3*Δ, *arb1*Δ, *arb2*Δ, *dcr1*Δ*rdp1*Δ, and *dcr1*Δ*tas3*Δ cell), and are reduced further in cells in which Ago1 is absent or cannot bind to small RNAs (about 20- to 40-fold reduction in *ago1*Δ and Ago1-3A cells) (Figure 5E). In further support of a role for priRNAs in H3K9 methylation, we observed a correlation between an increase in priRNA levels in *dcr1*Δ*cid14*Δ double-mutant cells (Figure 5F, Figure S5F) and increase in H3K9 methylation at the centromeric *dg* repeats (Figure 5G, Figure S5B). Ago1-mediated Dcr1-independent H3K9 methylation also correlated with a consistent reduction in centromeric noncoding RNA levels, which were about 1.4-fold more abundant in *ago1*Δ than in *dcr1*Δ cells (Figure S5G). These observations suggest that priRNAs act through Ago1 to nucleate H3K9 methylation at centromeric repeats.

Ago1-Bound Small RNAs Are Trimmed after Release of the Passenger Strand

We next explored possible mechanisms that may give rise to priRNAs. A clue to how these small RNAs may be generated came from analysis of siRNA sequences in *ago1*$^+$ cells expressing the Ago1-D580A mutant. Ago1-D580A contains ds-siRNAs because it fails to release the siRNA passenger strand and inhibits the spreading of H3K9 methylation in a dominant negative manner (Buker et al., 2007). We obtained near wild-type number of dg siRNA reads for FLAG-Ago1-D580 purifications from *ago1*$^+$ cells; however, the siRNAs mapping to the *dh*, *imr1*, and *IRC3* elements were greatly diminished (Figure 6A, Figures S6A and S6B, and data not shown). This defect is likely to be related to the interference of Ago1-D580A with the spreading of H3K9 methylation (Buker et al., 2007). Ago1-D580-associated small RNAs had the same 5′ nucleotide preference as wild-type Ago1 (Figure S6C), but in contrast to wild-type and most mutant backgrounds, which contained siRNAs of 21–23 nucleotides in size (e.g., Figure S4B), centromeric siRNAs associated with Ago1-D580A had a broader size distribution ranging from 21 to 27 nucleotides (Figure 6B). This increase in siRNA length was only observed for centromeric siRNAs, which are Dicer products and load onto Ago1 as double stranded, since Ago1-D580A had no effect on the size distribution of small RNAs corresponding to mRNAs and rRNAs (Figure S6D). Furthermore, centromeric siRNA sequences with identical 5′ ends were extended at their 3′ ends when associated with Ago1D580A (Figures 6C and 6D). These results suggest that Ago1 is able to bind to larger precursor small RNAs, which are then trimmed to ~22 nt siRNAs after release of the passenger strand, and raise the possibility that a similar trimming mechanism gives rise to mature priRNAs.

We next compared the frequency of mismatches at the 3′ ends of wild-type Ago1 and Ago1-D580A-bound siRNAs. As shown in Figure S6E, we observed similar numbers of 3′ end mismatches in the wild-type and mutant Ago1 proteins, suggesting that increased nucleotidyltransferase activity was not responsible for the larger size of siRNAs bound to Ago1-D580A. In addition, perfectly matched centromeric siRNAs, bound to Ago1-D580A, showed a similar broader length distribution as all centromeric siRNAs, further excluding increased nucleotidyltransferase activity as an explanation for larger size (Figure 6E). Together, these observations strongly suggest that Ago1-associated siRNAs are trimmed at their 3′ end by an unknown ribonuclease after the release of the passenger strand.

In *Drosophila* and vertebrate germline cells, the ping-pong amplification mechanism generates piRNAs using the slicer activity of two different Piwi family proteins (reviewed in Aravin et al., 2007; Ghildiyal and Zamore, 2009). We found that priRNA levels were comparable in Ago1-D580A and *dcr1*Δ cells

(F) Average genome-wide distribution of priRNAs mapping to chromosome 1 mRNAs in *dcr1*Δ cells. The coding region of each mRNA was divided to five equal parts, each representing 20% of the protein coding sequence. The 3′ untranslated region (UTR) and downstream regions were divided into windows of 50 and 100 nucleotides. The number of priRNA reads mapping to each window was normalized to the size of the corresponding window and to the total number of mRNAs. The number of priRNA reads represents normalized average number of reads per 1 kb window.

(G) Splinted ligation detection of centromeric small RNAs associated with Argonaute or from total RNA, showing that priRNAs are enriched in the Argonaute purification.

(H) Sybr Green II staining of 17.5% denaturing polyacrylamide gel with 3 μg of RNAs associated with FLAG-Ago1 or FLAG-Ago1-3A purified from *dcr1*Δ cells. RNAs of approximately 22 nt in length are specifically associated with wild-type FLAG-Ago1.

(I) Silencing assay showing that the expression of wild-type Ago1, but not Ago1-D580A or Ago1-3A (F276A/Y513A/K517A) mutants, rescues loss of silencing in *ago1*Δ cells. Growth on FOA medium indicates *ura4*$^+$ silencing.

(J) Splinted ligation detection of small RNAs associated with wild-type and mutant Ago1 proteins, showing that Ago1-3A containing three point mutations in the MID and PAZ domains abolishes small RNA binding. Ago1-F276A containing a single point mutation in the PAZ domain binds small RNAs more weakly. See also Figure S4.

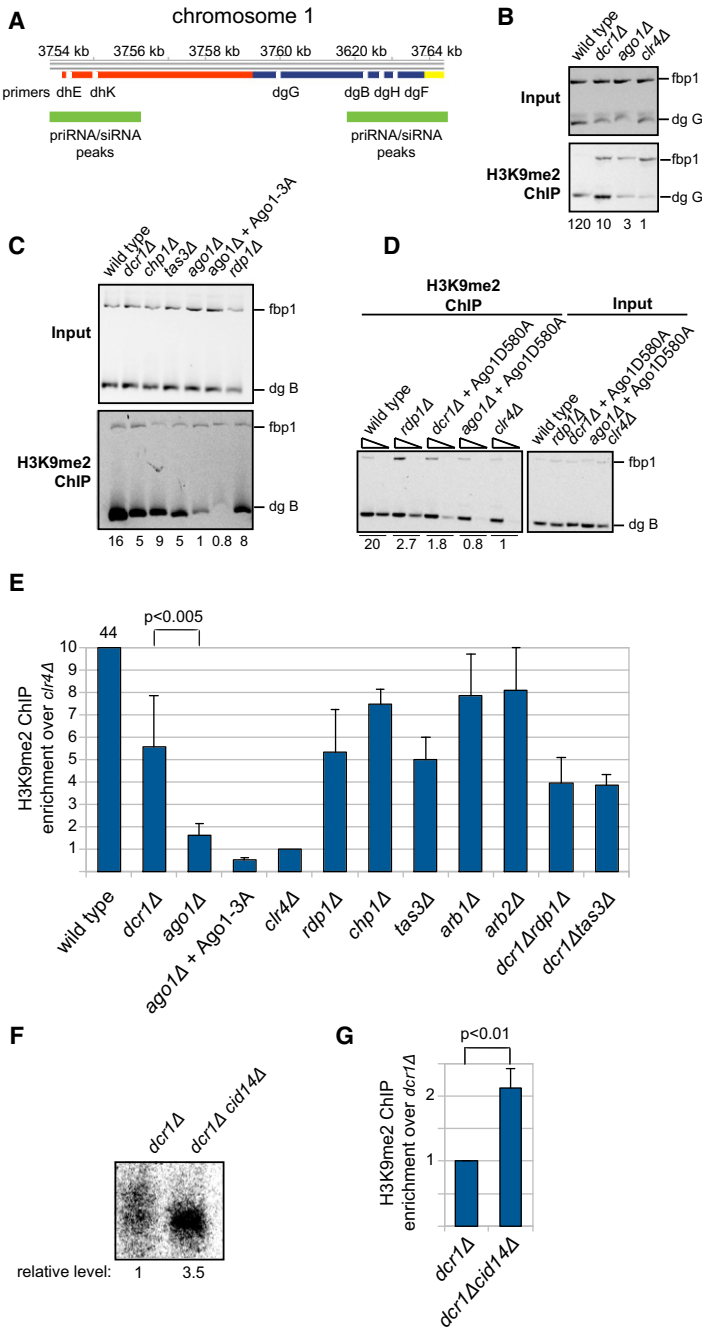

Figure 5. Role for priRNAs in Promoting Histone H3K9 Methylation

(A) Location of PCR products in ChIP and qRT-PCR experiments are indicated as white bars below the *dg* (blue), *dh* (red), and *imr1L* (yellow) regions of chromosome 1. Green bars depict regions with mapped siRNAs.

(B) Chromatin immunoprecipitation (ChIP) experiments showing Dcr1-independent and Ago1-dependent H3K9 methylation at the indicated centromeric *dgG* region (also see Figure S5). ChIP experiments were performed with H3K9me2 antibody. Relative fold enrichment over *clr4*Δ is indicated bellow each panel.

(C) ChIP experiments showing that priRNA/siRNAs can induce low level of H3K9 methylation independently of the Chp1 and Tas3 subunits of RITS. Ago1-3A mutant deficient in priRNA binding is unable to direct H3K9 methylation.

(D) ChIP experiments showing that slicer activity of Ago1 is essential for priRNA-dependent H3K9 methylation; serial dilutions containing 1 and 1/30th μl of immunoprecipitated DNA were used and the lower dilution, for which PCR is in the linear range for all samples, was used for quantification.

(E) Quantification of the ChIP data. ChIP experiments were performed several times with independent biological replicates and average values with standard deviation are shown as enrichment over *clr4*Δ. The average enrichment for wild-type, *dcr1*Δ, and *ago1*Δ was based on more than 15 experiments with different primers sets. p values were calculated using the Student's t test.

(F and G) Increase in priRNA levels correlates with increased H3K9 methylation. Splinted ligation detection of Argonaute-associated centromeric small RNAs showing that centromeric priRNAs are 3.5-fold more abundant in *dcr1*Δ*cid14*Δ than in *dcr1*Δ cells (F). Splinted ligation was performed as described in Figure 1. Quantification of ChIP experiments showing 2-fold higher levels of H3K9 methylation in *dcr1*Δ*cid14*Δ than in *dcr1*Δ. The dgB primers were used in this ChIP experiments and the results show the average for seven independent biological replicates. Error bars indicate standard deviations. p value was calculated using the Student's t test.

See also Figure S5.

(Figure 6F), indicating that a slicer-based mechanism was not involved in priRNA generation. In *C. elegans*, Dicer-independent secondary small RNAs are generated by RNA-directed RNA polymerases (Aoki et al., 2007). However, priRNA levels were similar in *dcr1*Δ and *dcr1*Δ*rdp1*Δ double-mutant cells, ruling out a role for Rdp1 in priRNA generation (Figure 6F). Furthermore, priRNA levels were not affected by deletion of *eri*$^{+}$, which encodes a double strand-specific ribonuclease (Iida et al., 2006), suggesting that priRNAs were single stranded and were generated from single-stranded precursor (Figure 6F). We also observed a correlation between the levels of specific centromeric transcripts and the levels of corresponding priRNAs (Figures S6F and S6G). For example, higher transcript levels from the (−) strand of the *dh* repeat (dhE region) correlated with higher (−) strand priRNA levels from the same region (Figures S6F and S6G).

The effect of Cid14, which is involved in targeting RNA for degradation or processing to the exosome, on both the frequency of siRNA 3′end mismatches (Figures 2E and 2F) and priRNA levels (Figure 5F) suggests that the degradation of small RNAs is at least partly mediated by the exosome. The exosome is essential for *S. pombe* viability, but mutations in the Dis3 subunit in the catalytic core of the exosome are viable, although they have a severe growth defect. To determine whether the exosome was required for priRNA generation or trimming, we sequenced FLAG-Ago1-bound small RNAs from *dis3-54,D171N dcr1*$^{+}$ and *dis3-54,D171N dcr1*Δ cells. The results showed that in *dis3-54,D171N dcr1*Δ mutant cells priRNAs were still present, although their levels were lower than in *dcr1*Δ cells (Figures 6F and 6G). siRNAs in *dis3-54,D171N dcr1*$^{+}$ cells had a similar size distribution as in wild-type cells, although 3% of siRNAs were several nucleotides longer, suggesting that Dis3/exosome might be involved in trimming of siRNAs

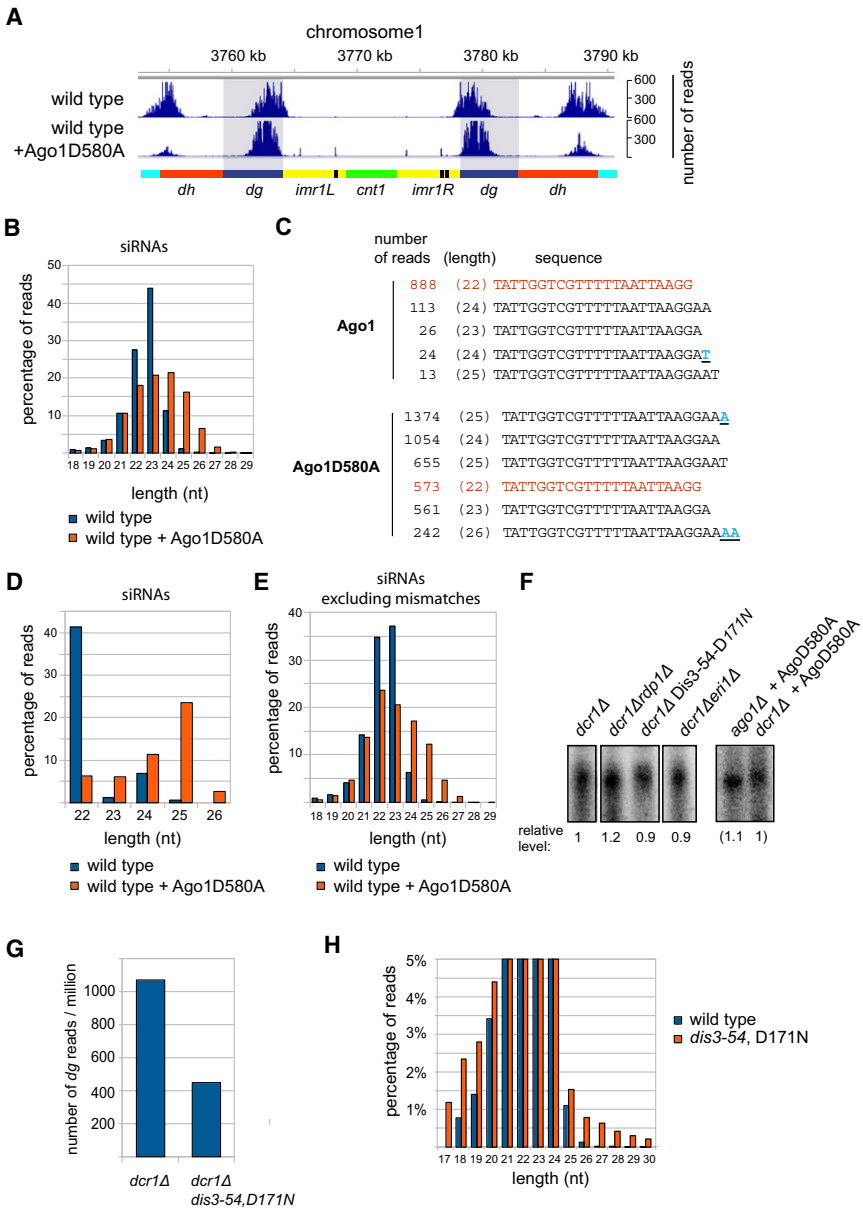

Figure 6. Ago1-Bound siRNAs Are Trimmed after Release of the Passenger Strand

(A) Small RNA reads in wild-type cells, with and without expression of the Ago1D580A dominant negative mutant, are plotted over centromeric repeat region of chromosome 1.

(B) Length distribution of centromeric siRNAs associated with Ago1 and Ago1-D580A, showing the broader siRNA length distribution of Ago1-D580A-associated siRNAs.

(C) Centromeric siRNAs with identical 5′ ends and different 3′ ends bound by Ago1 and Ago1-D580A. The number of reads and the length are indicated for each siRNA. Mismatched residues are shown in underlined blue.

(D) Length distribution of centromeric siRNAs from (C) with identical 5′ ends bound by Ago1 and Ago1-D580A. The siRNA is extended at its 3′ end in Ago1-D580A, suggesting that in wild-type Ago1 the siRNA is trimmed from its 3′ end.

(E) Length distribution of centromeric dg siRNAs that perfectly match the *S. pombe* genome associated with Ago1-D580A compared to the wild-type.

(F) Splinted ligation detection of Argonaute-associated centromeric small RNAs in indicated mutant cells. The levels of centromeric priRNAs are similar in *dcr1*Δ*rdp1*Δ, *dcr1*Δ*eri1*Δ and *dcr1*ΔDis3-54,D171N mutant cells. Splinted ligation detection was performed as described in Figure 1.

(G) Number of priRNA reads normalized to one million reads mapping to *dg* in *dcr1*Δ and *dcr1*Δ*dis3-54*,D171N mutant cells. priRNAs are approximately 2-fold more abundant in *dcr1*Δ than in *dcr1*Δ*dis3-54*,D171N mutant cells.

(H) Size distribution of centromeric siRNAs associated with Ago1 in wild-type and *dis3-54*,D171N mutant cells. Approximately 3% of total siRNAs have a larger average size in *dis3-54*,D171N mutant cells compared to the wild-type cells.

See also Figure S6.

(Figure 6H). Moreover, in the *dis3* mutant cells, we observed an increase in the number of priRNAs corresponding to mRNAs and tRNAs (compare Figure 2A with Figure S6H), which provides further support for the idea that Ago1 acts as a receptor for genome-wide RNA degradation products. However, priRNA presence and a similar average size distribution, suggest that either residual exoribonuclease activity in *dis3-54*,*D171N* mutant cells is sufficient for priRNA generation or that the exosome acts redundantly with other ribonucleases in generating priRNAs.

DISCUSSION

Our findings reveal the existence of a distinct class of small RNAs (priRNAs), which are produced independently of Dicer or RDRC and mediate low levels of H3K9 methylation at the centromeric repeat sequences. priRNAs are likely to accumulate through the binding of RNA degradation products to Ago1 and may achieve their final size through a trimming/protection mechanism, which also applies to Dicer-dependent centromeric siRNAs (Figure 7). Our results also provide a mechanism for the nucleation of siRNA amplification on specific centromeric transcripts in the initial absence of heterochromatin or Dicer-generated siRNAs and demonstrate a key role for the small RNA binding and slicer activities of Ago1 in siRNA amplification. These findings have implications for the roles of Argonaute family proteins in transcriptome surveillance and suggest possible parallels between Argonautes and major histocompatibility (MHC) antigen receptors in transcriptome and proteome surveillance, respectively.

Biogenesis of Small RNAs from Centromeric Repeats

Our observations suggest that two major Ago1-dependent pathways mediate the initial generation of small RNAs in a heterochromatin-independent manner (Figure 7).

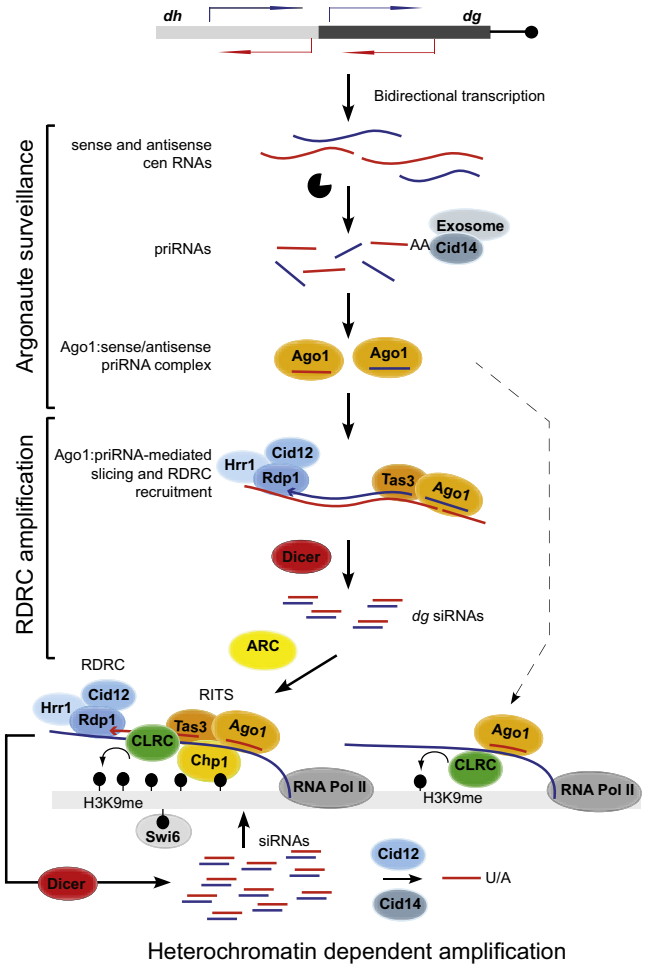

Figure 7. Model for Initiation of siRNA Generation and Heterochromatin Assembly

Model summarizing pri/siRNA generation and amplification in heterochromatin-independent and heterochromatin-dependent manners. priRNAs are generated by degradation of centromeric transcripts and loaded onto Ago1. priRNAs target centromeric transcripts and induce heterochromatin independent siRNA generation in an Ago1 slicer- and RDRC/Dicer-dependent manner. Amplified siRNAs target nascent transcripts, recruit RITS, RDRC, and CLRC complexes to induce efficient siRNA amplification and H3K9 methylation. The ARC complex is required for this heterochromatin-dependent amplification step. priRNAs can also target chromatin bound nascent centromeric transcripts (dashed arrow), recruit the CLRC complex, and induce low levels of H3K9 methylation generation. The Cid12 and Cid14 nucleotidyltransferase enzymes modify the 3′ ends of small RNAs, leading to exosome-mediated trimming or degradation. CLRC, Clr4 H3K9 methyltransferase complex; black lollipops, H3K9 methylation.

First, bidirectional transcription from centromeric repeats results in the accumulation of RNA degradation products of diverse sizes that bind to Ago1. This binding reflects the ability of Ago1 to associate with nearly all cellular RNA degradation products in a manner that appears to be proportional to their abundance and linked to transcription termination or 3′ end processing. This includes rRNA, tRNA, and mRNA degradation products that have also been observed to associate with Argonaute family members from other organisms in several previous studies. Despite this general association, siRNA amplification and heterochromatin formation are limited to specific genomic regions such as pericentromeric repeats. We propose that the basis of this specificity lies partly in the prevalence of bidirectional transcription within centromeric repeats, which generates both sense and antisense transcripts. Whereas priRNAs cannot target most genomic regions containing protein coding genes and non-repetitive sequences, they can readily target repetitive regions that are bidirectionally transcribed because priRNAs will have antisense targets within these regions (Figure 7).

Second, our results demonstrate that heterochromatin-independent amplification of siRNAs occurs only on dg centromeric transcripts. Although specific structural features in dg RNAs are likely to be important, dg siRNA amplification requires the slicer activity of Ago1 (Figure 3D), which suggests that Ago1 participates in targeting the dg RNA and has to be loaded with a small RNA prior the amplification. Ago1, guided by the small RNA, must target the dg RNA before dsRNA synthesis by RDRC can commence (Figure 7). This is consistent with the ability of RDRC to load onto the free 3′ end of target RNA molecules in vitro (Motamedi et al., 2004). Previously, we have shown that the RITS and RDRC complexes coimmunoprecipitate. Our present results show that the Tas3, but not the Chp1, subunit of RITS is required for heterochromatin-independent siRNA amplification, suggesting that an Ago1/Tas3 subcomplex targets RDRC to dg RNAs (Figure 7).

Once heterochromatin-independent dg siRNAs accumulate, the RITS complex targets centromeric transcripts to induce both H3K9 methylation and siRNA amplification at the *dg* repeat regions. High levels of H3K9 methylation and siRNAs at *dg* repeats are then likely to nucleate the spreading of RNAi and heterochromatin to adjacent regions (Figure 7, bottom).

Thus, contrary to expectations, our results suggest that a Dicer and RDRC-independent Ago1 surveillance mechanism, rather than the processing of dsRNA formed from centromeric sense and antisense transcripts, mediates the nucleation of RNAi and heterochromatin assembly at the fission yeast pericentromeric repeats. Although some initial small RNAs might also originate from Dicer processing of dsRNA, as has been proposed to occur at convergently transcribed genes (Gullerova and Proudfoot, 2008), the similar levels of small RNAs and H3K9 methylation in *dcr1*Δ and *rdp1*Δ cells (Figure 1 and 5C), respectively, suggest that this pathway is inefficient and does not significantly contribute to the overall levels of Ago1-associated centromeric small RNAs in *rdp1*Δ cells.

priRNA Biogenesis

Our observation that centromeric siRNAs associated with Ago1-D580A in *ago1*$^{+}$ cells had a broader length distribution suggests that the 3′ ends of Ago1-bound small RNAs are trimmed by an unknown ribonuclease. Since the *S. pombe* Dicer generates dsRNA products of diverse sizes (20–30nt) (Colmenares et al., 2007), trimming may be necessary to reduce siRNA length, which might be critical for proper siRNA binding to Ago1 or for proper interaction with the target RNA. We propose that Argonaute also binds to random degradation products of abundant RNAs, which are further trimmed to 22–23 nucleotide priRNAs by a similar mechanism to the siRNA trimming described above. Our results suggest that the exosome is at least partially

responsible for small RNA 3′ end formation in *S. pombe*, as a small fraction of Ago1-bound small RNAs in a hypomorphic exosome mutant is slightly larger than small RNAs in wild-type cells. It has also been speculated that exonucleases are involved in vertebrate piRNA 3′ end formation (Aravin et al., 2007; Ghildiyal and Zamore, 2009). However, future studies are required to determine the identity(ies) of the ribonucleases that mediate priRNA generation.

Implications for Argonaute-Mediated Transcriptome Surveillance

Repetitive DNA elements and transposons form the bulk of the genomes of many metazoan organisms. The mobility and activity of these elements is often curtailed by RNA silencing mechanisms that are thought to act on aberrant transcripts. It is unclear how aberrant transcripts are recognized, but the mechanism appears to involve competition between different RNA processing pathways. Our observations raise the possibility that Argonaute surveillance may play a widespread role in initiation of RNA silencing. Bidirectional transcription of DNA repeats and transposons would produce sense and antisense transcripts, which may be degraded in the nucleus to generate threshold levels of antisense small RNAs. These small RNAs would then target Argonaute to cytoplasmic or chromatin-bound transcripts to mediate small RNA amplification and silencing. In fission yeast, plants, and *C. elegans*, the amplification step involves RDRC and Dicer-based mechanisms (see Figure 7), whereas in the case of piRNAs in fly and vertibrate germ cells, the amplification step appears to be carried out by the ping-pong mechanism rather than RDRC/Dicer (Aravin et al., 2007; Farazi et al., 2008; Ghildiyal and Zamore, 2009). In this regard, the surveillance activity of Argonaute is reminiscent of the major histocompatibility antigen receptors, which act in proteome surveillance by binding and presenting protein degradation products (Trombetta and Mellman, 2005).

EXPERIMENTAL PROCEDURES

Protein Affinity Purification, RNA Synthesis, and Cid12 Activity Assays

Proteins were purified with affinity chromatography from *S. pombe* and *E. coli* cells. Rdp1 and Cid12 activity was reconstituted by the addition of FLAG-purified Rdp1, Hrr1, and Cid12 to a T7-generated single-stranded RNA template or RNA oligonucleotide. The reaction was incubated at 37°C or 30°C for 1–2 hr and analyzed on 10%–17% polyacrylamide gels under either denaturing or native conditions. See the Extended Experimental Procedures for detailed protocol. Oligonucleotides used in RDRC activity assays are listed in Table S2.

siRNA Purification and Detection

siRNAs associated with Ago1 were purified from cells expressing Flag-Ago1 from a pREP1 plasmid by immunoaffinity purification of FLAG-Ago1 with an M2 affinity resin (Sigma) (Buker et al., 2007). siRNAs were recovered from FLAG-Ago1 by phenol-chloroform extraction and ethanol precipitation and detected by the splinted ligation method as described (Maroney et al., 2008). In the splinted ligation assay, a radioactively labeled oligonucleotide was mixed with a bridge oligonucleotide and input small RNAs. Reactions were denatured followed by annealing for 10 min. Small RNA and ligation oligonucleotide annealed to bridge oligonucleotide were ligated with T4 DNA ligase (NEB) for 1 hr. Excess of radioactively labeled ligation oligonucleotide was dephosphorylated with CIP phosphatase (NEB). Reactions were then run on a 17% polyacrylamide gel, and ligated products were detected with phosphorimager. See Figure S1A for schematic illustration. Oligonucleotides used for siRNA detection are listed in Table S2. See the Extended Experimental Procedures for detailed protocol.

Strain Construction

S. pombe strains used in this study are described in Table S3. Plasmids used in this study are listed in Table S4.

Chromatin Immunoprecipitation

ChIP was performed as described previously (Huang and Moazed, 2003). Dimethylated H3-K9 (H3K9me2, Abcam number Ab1220) antibody was used for immunoprecipitation. Oligonucleotides used in ChIP assays are listed in Table S2. See the Extended Experimental Procedures for detailed protocol.

Statistical Methods

Statistical significance was calculated with the Student's t test.

Small RNA Libraries

Gel-purified and size-selected (18–30 nucleotide) Ago1-associated RNAs were incubated with preadenylated 3′-adaptor oligonucleotide in a ligation buffer without ATP at 20°C for 2 hr. The 3′ ligation reaction was purified on a 17% polyacrylamide gel. For the 5′ ligation, 3′ ligated products were incubated with 5′ adaptor oligonucleotide at 20°C for 2 hr. The ligated reaction was gel purified and used for first-strand complementary DNA (cDNA) synthesis. cDNA was amplified with PCR with Illumina P5 and P7 oligos for 10–15 cycles and gel purified. See the Extended Experimental Procedures for references and a detailed protocol.

Analysis of Sequencing Data

Small RNA sequencing data sets generated in this study are listed in Table S1. Illumina small RNA reads which matched to the first 6 nt of the 3′ linker were selected. Reads of 18–29 nt in size were mapped to the *S. pombe* genome, allowing a 3 nt mismatch to the genome with Maq (http://maq.sourceforge.net/) and/or Novoalign (http://www.novocraft.com/). Small RNA reads mapping to multiple locations were randomly assigned. Two mismatches were allowed in the final selection of small RNA. Small RNA reads were normalized to one million small RNAs. Scripts used for processing of the data are available upon request. We used the genome sequence and annotation that were available from the *S. pombe* Genome Project (http://www.sanger.ac.uk/Projects/S_pombe/). The data are displayed with Integrative Genomics Viewer (IGV) (http://www.broad.mit.edu/igv/).

ACCESSION NUMBERS

The small RNA sequences reported in this paper has been deposited in the NCBI Gene Expression Omnibus with the accession number GSE19734.

SUPPLEMENTAL INFORMATION

Supplemental Information includes Extended Experimental Procedures, five figures, and four tables and can be found with this article online at doi:10.1016/j.cell.2010.01.019.

ACKNOWLEDGMENTS

We thank members of the Moazed lab for helpful discussions, Aaron Johnson, Daniel Holoch, Geng Li, and Silvija Bilokapic for comments on the manuscript, and Serafin Colmenares for the observation that Rdp1 overexpression suppresses the requirement for Cid12. This work was supported by an EMBO long-term fellowship to M.H. and a grant from the National Institutes of Health to D.M. (GM72805). D.M. is a Howard Hughes Medical Institute investigator.

Received: September 1, 2009
Revised: November 16, 2009
Accepted: January 6, 2010
Published: February 18, 2010

REFERENCES

Aoki, K., Moriguchi, H., Yoshioka, T., Okawa, K., and Tabara, H. (2007). In vitro analyses of the production and activity of secondary small interfering RNAs in C. elegans. EMBO J. *26*, 5007–5019.

Aravin, A.A., Hannon, G.J., and Brennecke, J. (2007). The Piwi-piRNA pathway provides an adaptive defense in the transposon arms race. Science *318*, 761–764.

Baulcombe, D. (2004). RNA silencing in plants. Nature *431*, 356–363.

Bühler, M., Verdel, A., and Moazed, D. (2006). Tethering RITS to a nascent transcript initiates RNAi- and heterochromatin-dependent gene silencing. Cell *125*, 873–886.

Bühler, M., Haas, W., Gygi, S.P., and Moazed, D. (2007). RNAi-dependent and -independent RNA turnover mechanisms contribute to heterochromatic gene silencing. Cell *129*, 707–721.

Bühler, M., Spies, N., Bartel, D.P., and Moazed, D. (2008). TRAMP-mediated RNA surveillance prevents spurious entry of RNAs into the Schizosaccharomyces pombe siRNA pathway. Nat. Struct. Mol. Biol. *15*, 1015–1023.

Buker, S.M., Iida, T., Bühler, M., Villén, J., Gygi, S.P., Nakayama, J., and Moazed, D. (2007). Two different Argonaute complexes are required for siRNA generation and heterochromatin assembly in fission yeast. Nat. Struct. Mol. Biol. *14*, 200–207.

Cam, H.P., Sugiyama, T., Chen, E.S., Chen, X., FitzGerald, P.C., and Grewal, S.I. (2005). Comprehensive analysis of heterochromatin- and RNAi-mediated epigenetic control of the fission yeast genome. Nat. Genet. *37*, 809–819.

Chen, C.C., Simard, M.J., Tabara, H., Brownell, D.R., McCollough, J.A., and Mello, C.C. (2005). A member of the polymerase beta nucleotidyltransferase superfamily is required for RNA interference in C. elegans. Curr. Biol. *15*, 378–383.

Colmenares, S.U., Buker, S.M., Buhler, M., Dlakić, M., and Moazed, D. (2007). Coupling of double-stranded RNA synthesis and siRNA generation in fission yeast RNAi. Mol. Cell *27*, 449–461.

Debeauchamp, J.L., Moses, A., Noffsinger, V.J., Ulrich, D.L., Job, G., Kosinski, A.M., and Partridge, J.F. (2008). Chp1-Tas3 interaction is required to recruit RITS to fission yeast centromeres and for maintenance of centromeric heterochromatin. Mol. Cell. Biol. *28*, 2154–2166.

Farazi, T.A., Juranek, S.A., and Tuschl, T. (2008). The growing catalog of small RNAs and their association with distinct Argonaute/Piwi family members. Development *135*, 1201–1214.

Ghildiyal, M., and Zamore, P.D. (2009). Small silencing RNAs: an expanding universe. Nat. Rev. Genet. *10*, 94–108.

Gullerova, M., and Proudfoot, N.J. (2008). Cohesin complex promotes transcriptional termination between convergent genes in *S. pombe*. Cell *132*, 983–995.

Hammond, S.M., Bernstein, E., Beach, D., and Hannon, G.J. (2000). An RNA-directed nuclease mediates post-transcriptional gene silencing in Drosophila cells. Nature *404*, 293–296.

Hannon, G.J. (2002). RNA interference. Nature *418*, 244–251.

Henderson, I.R., and Jacobsen, S.E. (2007). Epigenetic inheritance in plants. Nature *447*, 418–424.

Huang, J., and Moazed, D. (2003). Association of the RENT complex with nontranscribed and coding regions of rDNA and a regional requirement for the replication fork block protein Fob1 in rDNA silencing. Genes Dev. *17*, 2162–2176.

Hutvagner, G., and Simard, M.J. (2008). Argonaute proteins: key players in RNA silencing. Nat. Rev. Mol. Cell Biol. *9*, 22–32.

Iida, T., Kawaguchi, R., and Nakayama, J. (2006). Conserved ribonuclease, Eri1, negatively regulates heterochromatin assembly in fission yeast. Curr. Biol. *16*, 1459–1464.

Lee, S.R., Talsky, K.B., and Collins, K. (2009). A single RNA-dependent RNA polymerase assembles with mutually exclusive nucleotidyl transferase subunits to direct different pathways of small RNA biogenesis. RNA *15*, 1363–1374.

Maroney, P.A., Chamnongpol, S., Souret, F., and Nilsen, T.W. (2008). Direct detection of small RNAs using splinted ligation. Nat. Protoc. *3*, 279–287.

Mello, C.C., and Conte, D., Jr. (2004). Revealing the world of RNA interference. Nature *431*, 338–342.

Moazed, D. (2009). Small RNAs in transcriptional gene silencing and genome defence. Nature *457*, 413–420.

Motamedi, M.R., Verdel, A., Colmenares, S.U., Gerber, S.A., Gygi, S.P., and Moazed, D. (2004). Two RNAi complexes, RITS and RDRC, physically interact and localize to noncoding centromeric RNAs. Cell *119*, 789–802.

Motamedi, M.R., Hong, E.J., Li, X., Gerber, S., Denison, C., Gygi, S.P., and Moazed, D. (2008). HP1 proteins form distinct complexes and mediate heterochromatic gene silencing by nonoverlapping mechanisms. Mol. Cell *32*, 778–790.

Noma, K., Sugiyama, T., Cam, H., Verdel, A., Zofall, M., Jia, S., Moazed, D., and Grewal, S.I. (2004). RITS acts in cis to promote RNA interference-mediated transcriptional and post-transcriptional silencing. Nat. Genet. *36*, 1174–1180.

Pak, J., and Fire, A. (2007). Distinct populations of primary and secondary effectors during RNAi in C. elegans. Science *315*, 241–244.

Partridge, J.F., Scott, K.S., Bannister, A.J., Kouzarides, T., and Allshire, R.C. (2002). cis-acting DNA from fission yeast centromeres mediates histone H3 methylation and recruitment of silencing factors and cohesin to an ectopic site. Curr. Biol. *12*, 1652–1660.

Sadaie, M., Iida, T., Urano, T., and Nakayama, J. (2004). A chromodomain protein, Chp1, is required for the establishment of heterochromatin in fission yeast. EMBO J. *23*, 3825–3835.

Schalch, T., Job, G., Noffsinger, V.J., Shanker, S., Kuscu, C., Joshua-Tor, L., and Partridge, J.F. (2009). High-affinity binding of Chp1 chromodomain to K9 methylated histone H3 is required to establish centromeric heterochromatin. Mol. Cell *34*, 36–46.

Sijen, T., Fleenor, J., Simmer, F., Thijssen, K.L., Parrish, S., Timmons, L., Plasterk, R.H., and Fire, A. (2001). On the role of RNA amplification in dsRNA-triggered gene silencing. Cell *107*, 465–476.

Sijen, T., Steiner, F.A., Thijssen, K.L., and Plasterk, R.H. (2007). Secondary siRNAs result from unprimed RNA synthesis and form a distinct class. Science *315*, 244–247.

Smardon, A., Spoerke, J.M., Stacey, S.C., Klein, M.E., Mackin, N., and Maine, E.M. (2000). EGO-1 is related to RNA-directed RNA polymerase and functions in germ-line development and RNA interference in C. elegans. Curr. Biol. *10*, 169–178.

Tomari, Y., Du, T., Haley, B., Schwarz, D.S., Bennett, R., Cook, H.A., Koppetsch, B.S., Theurkauf, W.E., and Zamore, P.D. (2004). RISC assembly defects in the Drosophila RNAi mutant armitage. Cell *116*, 831–841.

Trombetta, E.S., and Mellman, I. (2005). Cell biology of antigen processing in vitro and in vivo. Annu. Rev. Immunol. *23*, 975–1028.

Verdel, A., Jia, S., Gerber, S., Sugiyama, T., Gygi, S., Grewal, S.I., and Moazed, D. (2004). RNAi-mediated targeting of heterochromatin by the RITS complex. Science *303*, 672–676.

Volpe, T.A., Kidner, C., Hall, I.M., Teng, G., Grewal, S.I., and Martienssen, R.A. (2002). Regulation of heterochromatic silencing and histone H3 lysine-9 methylation by RNAi. Science *297*, 1833–1837.

Wang, S.W., Stevenson, A.L., Kearsey, S.E., Watt, S., and Bähler, J. (2008a). Global role for polyadenylation-assisted nuclear RNA degradation in posttranscriptional gene silencing. Mol. Cell. Biol. *28*, 656–665.

Wang, Y., Sheng, G., Juranek, S., Tuschl, T., and Patel, D.J. (2008b). Structure of the guide-strand-containing argonaute silencing complex. Nature *456*, 209–213.